

# Pick to place trajectories in human arm training environment

Jaka Zihnerl\*, Janez Podobnik, Mario Sikic and Marko Munih

*Laboratory of Robotics and Biomedical Engineering, Faculty of Electrical Engineering, University of Ljubljana, Ljubljana, Slovenia*

Received in final form 1 April 2009

**Abstract.** This paper presents a new method of trajectory planning in rehabilitation robotics. First were measured in healthy subject the pick to place trajectories while haptic robot is in zero impedance space. B-spline approximation is used to mathematically define the measured paths. This trajectory path serves as a central line for the rounding haptic tunnel. In addition to radial elastic and damping force an optional guidance force can be applied along the tunnel to reach the place point. The B-spline control points were observed around the robot and arm workspace. The trajectory path defined with B-splines is compared with minimum jerk and minimum torque defined trajectories. Finally are compared the pick to place movements with and without tunnel use in healthy subject and in stroke hemiplegic patient.

Keywords: Trajectory planning, haptic interface, rehabilitation robotics

## 1. Introduction

The demographic structure of population in developed countries shows an increasing number of older people [1]. Among them the stroke is a leading cause of disability [2], to a large extent affecting the activities of daily living [4]. A numbers of controlled trials showed that enhanced physical therapy improves recovery after a stroke [19]. This fact confirms a growing necessity of rehabilitation approaches. The progress in robotics introduced the robots into rehabilitation environment, beside human therapists. In rehabilitation robotics the haptic interfaces combined with virtual reality largely improve the patient's motivation [13].

Several systems have been developed for robotic training of upper and lower extremities. Training systems for upper extremities are divided into two groups: end effectors and exoskeletons [17]. Examples of exoskeleton devices include L-Exos [8], RUPERT [9], Pneu-WREX [21], CADEN-7 [15], The Intelligent Robotic Arm [22] and the latest design ARMin [14]. End effector upper extremity devices are more common. MIT-MANUS [10] with SCARA configuration allows planar movements as the patient plays simple video games. The MIME [11] system uses a Puma 560 robot manipulator which allows movement in three-dimensional space. A six-axis sensor measures the forces and torques between the

---

\*Address for correspondence: Jaka Zihnerl, Laboratory of Robotics and Biomedical Engineering, Faculty of Electrical Engineering, University of Ljubljana, Trzaska c. 25, 1001 Ljubljana, Slovenia. Tel.: +386 1 4768 485; Fax: +386 1 4768 239; E-mail: jaka.zihnerl@robo.fe.uni-lj.si.

robot and the patient. The Gentle/G [12] system based on the Gentle/S rehabilitation robot HapticMASTER includes reach and grasp tasks, correcting movements that stray too far from the correct pathway. The robot system for upper limbs rehabilitation developed by Deneve et al. [3] also belongs to the class of end-effector based robots. Impedance control and the upper limit of the position error are used to avoid a large movement deviation from the desired trajectory. Mihelj et al. [13] proposed a controller that uses the minimal intervention principle. The controller allows the patient more freedom in choosing the movement path. The patient only needs to reach a specified final posture.

Human arm movement from point to point is important movement primitive in robotic rehabilitation. Different studies showed the rules that characterize measured human movement [6,7,20]. These rules are used as a natural movement bound. Flash and Hogan [7] suggest that human chosen trajectories have minimum jerk change along the path. Shape of the path from point to point in this case is linear, which is rather unnatural. On the other side, Wada et al. [20] present path planning with minimum torque change. In opposition to the Flash and Hogan model, which is a kinematic criterion, the minimum torque model is a dynamic criterion.

This paper proposes trajectory shape planning using B-splines. The movements measured in healthy subjects are used for trajectory approximation with B-splines [5]. These are used for new haptic object, a trajectory tunnel, that enables movement from pick to place point along a desired trajectory in a virtual haptic environment. The bisector of the tunnel and radius of the tunnel are generated using B-splines and control points. The trajectory tunnel is developed as an independent haptic primitive in virtual tasks. Subject's arm is placed in a fixture on the end effector of the haptic robot HapticMaster that is used as a force measurement and position generation device.

## 2. Methods

### 2.1. Haptic system specification

The rehabilitation system used in the study consists of the haptic interface device HapticMaster (Moog FCS Inc.), a wrist connection mechanism, a grasping device, a lower and upper arm gravity compensation mechanism, a 3D visualization system and a Dolby surround sound display. The robot and the grasping device are shown in Fig. 1.

The HapticMaster is a three degrees of freedom admittance controlled haptic interface. It is used as a force measuring device and as a feedback position generator. Podobnik [16] developed a device that enables the measurement of the grasp force. A gimbal with two passive degrees of freedom allows reorientation of the subject's hand. The system is upgraded with a one degree of freedom finger opening and closing subsystem in order to provide grasping, reaching, and object carrying capabilities. The described upper limb rehabilitation system allows training of complex activities of daily living in an adaptive virtual environment. The 3D virtual environment is projected in front of the patient via two LCD projectors.

Two subjects participated in the study. The first subject is a right handed, 24 years old healthy male. This participant had no history of neuromuscular or musculoskeletal disorders related to the upper extremities. The second participant is a right-hemiparetic subject, 40 years old female. Both subjects gave their informed consent to participate.

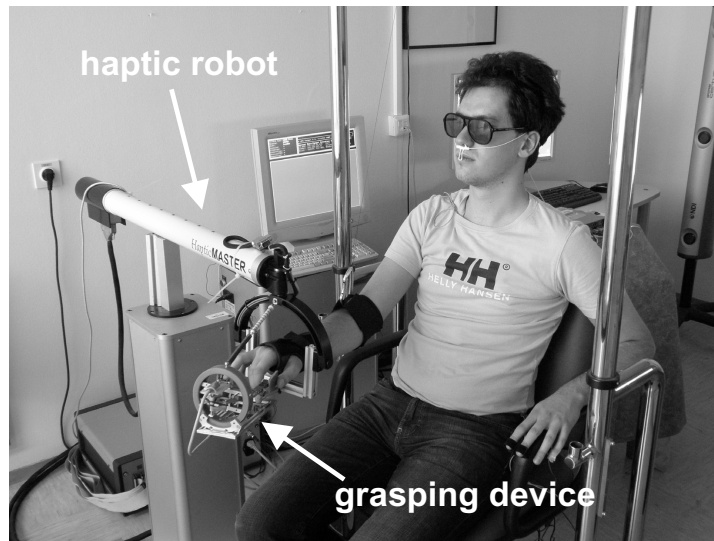


Fig. 1. Subject training with haptic system: a grasping device is attached to the HapticMaster end-effector, a 3D projection screen is positioned in front of the subject.

## 2.2. Trajectory planning

Pick to place human movement from point to point in 3D space, including pick, transfer and release of the objects is of utmost priority in everyday life and as such the basis in robotic rehabilitation of upper extremities. Studies of the movements measured indicate several rules:

1. The path of the arm is curved from pick to place points and slightly deviates from a straight line. Slight curvature does occur, depending on the area of the arm's workspace [7,18].
2. The velocity profile is bell-shaped. Human chooses the trajectory with the minimum jerk change of the hand. The acceleration profile of the movement contains no discontinuities [7].
3. The accuracy of the movement is inversely proportioned to the movement velocity. The relationship is known as Fitts' law [6].
4. The path is the most curved, where the velocity is the least [18].

Movements of the arm are becoming smoother and more elegant with exercise and learning. The smoothness of the movements is described [7] using the time derivative of the trajectory. Flash and Hogan suggested the third derivative in the minimum jerk model [7]. Among all trajectories, the one which minimizes the following functional is chosen:

$$C_1 = \frac{1}{2} \int_0^{T_f} \left( \left( \frac{d^3x}{dt^3} \right)^2 + \left( \frac{d^3y}{dt^3} \right)^2 + \left( \frac{d^3z}{dt^3} \right)^2 \right) dt. \quad (1)$$

Similar to the minimal jerk model is the minimal angle jerk model [20]. A trajectory based on the minimum angle jerk criterion (2) minimizes the angle jerk:

$$C_2 = \frac{1}{2} \int_0^{T_f} \sum_i \left( \frac{d^3\theta_i}{dt^3} \right)^2 dt. \quad (2)$$

$T_f$  represents the complete time of the movement and  $\theta_i$  represents the angle. As an opposite to the minimum jerk model, Wada et al. [20] suggest the minimum torque model, where the dynamics of the human arm is included. This model searches for a trajectory, where the change of the torque  $\tau_i$  is minimal. Model chooses the trajectory which minimizes the functional:

$$C_3 = \frac{1}{2} \int_0^{T_f} \sum_i \left( \frac{d\tau_i}{dt} \right)^2 dt. \quad (3)$$

A minimum variance model [18] provides a biological basis for the criteria it optimizes. Here, the variance of the hand position  $\sigma_i$  at the end of the movement is minimized, given that the control signals of the arm's actuators are subject to random noise with zero mean:

$$C_4 = \sum_{n=T+1}^{T+N-1} \left( (\sigma_x^2)^2 + (\sigma_y^2)^2 \right). \quad (4)$$

The minimum jerk model generates point to point trajectories whose paths are straight lines and whose velocity profiles are bell-shaped with a single peak. The trajectories generated by the dynamic model are curved with bell-shaped velocity profiles. The point to point movement trajectory planned by minimum angle jerk model is a straight path in the joint space and gradually curved in the Cartesian coordinate. The trajectories of the minimum variance model and minimum angle jerk model are very similar to those of the minimum torque change model, although the velocity profiles of minimum variance model slightly differ.

### 2.3. Realization of the pick to place trajectory using B-splines

In this subsection is described how movements were measured and then approximated by using B-splines.

For the trajectory path measurement was developed a simple task which included a block object on the floor and a table. The healthy subject had to pick the object and place it on the table. After successful placing, the object reappeared at a random starting point on the virtual floor. The subject was seating comfortably in a chair in front of the robot workspace and was instructed to grasp the handle. The placing end point was always at the center of the table, which was 7 cm above the virtual floor. Figure 2 shows twelve approximated trajectories of the pick to place movements in  $\vec{y}\vec{z}$  plane. The movements were made in zero impedance robot mode. This set of the measured movements represents a reference pick to place trajectories. The movements lengths varies from 20 to 45 cm in the horizontal direction while the vertical direction height is 7 cm.

On the basis of measured reference path trajectory, is generated a mathematically determined path trajectory combined with B-splines, which are used for local approximation and later interpolation of the measured movements with lower degree polynomials. The splines are used as basic functions which are smooth at contact points between segments. Contact points are also known as knots (Fig. 3a).

Let  $x_0 < x_1 < \dots < x_n$  represent the knots, selected along the trajectory, while  $b_{i,l}$  marks the  $i$ -th basic spline with  $l$  degree in the knots  $\{x_j\}_{j=0}^n$ . Choosing the knots  $x_{-l} < x_{-l+1} < \dots < x_0$  and  $x_n < x_{n+1} < \dots < x_{n+l}$ , a set can be defined:

$$b_{j,0}(x) = \begin{cases} 1, & x \in [x_j, x_{j+1}) \\ 0, & \text{otherwise} \end{cases} \quad (5)$$

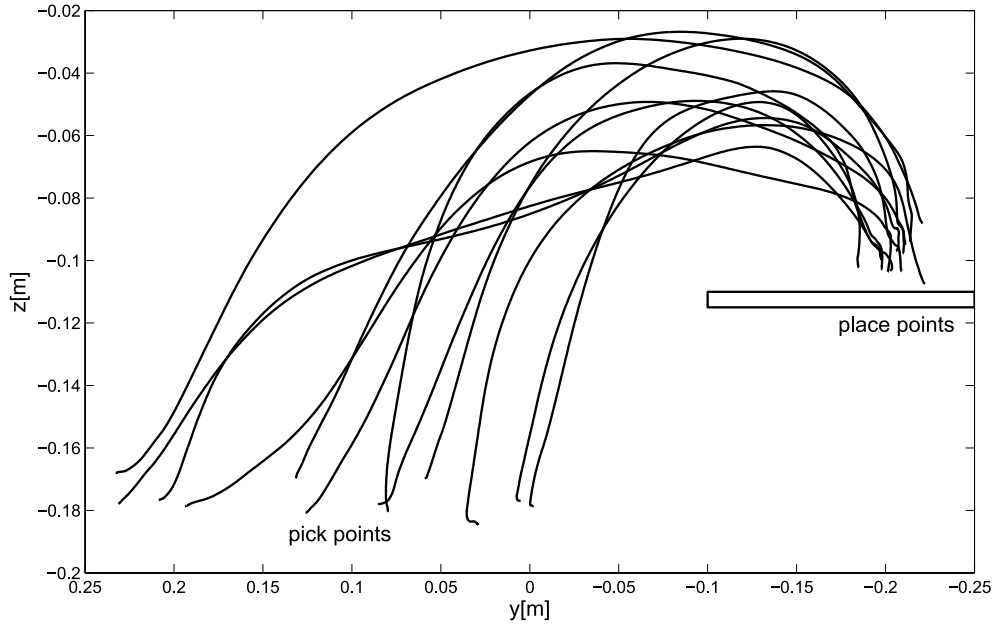


Fig. 2. Pick to place movements in the vertical yz plane. The healthy subject had to pick an object from the floor and place it on the table.

$$b_{j,k}(x) = \frac{x - x_j}{x_{j+k} - x_j} b_{j,k-1}(x) + \frac{x_{j+k+1} - x}{x_{j+k+1} - x_{j+1}} b_{j+1,k-1}(x) \quad (6)$$

The defined set  $\{b_{j,k}(x)\}$  is the base of the splines vector space with the knots  $x_0, \dots, x_n$  and degree  $k$ . The whole function  $s(x)$  is sum of functions

$$s(x) = \sum_{j=0}^{n-k-1} d_j b_{j,k}(x) \quad x \in [x_k, x_{n-k}], \quad (7)$$

where  $d_j$  are control points and the function  $s(x)$  is defined on the interval  $[x_k, x_{n-k}]$ . The control points are coefficients of the approximation with basic functions. DeBoor's algorithm [5] is suitable and simple for calculating the function  $s(x)$ . DeBoor's algorithm enables fast calculation and is numerically stable:

$$x \in [x_l, x_{l+1}] \quad (8)$$

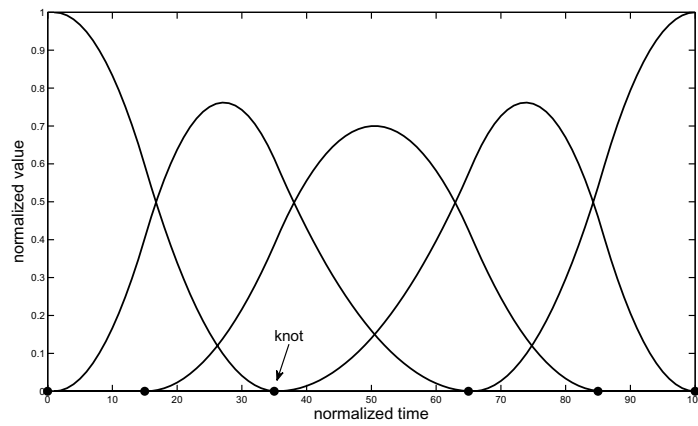
$$d_j^{[0]} = d_j \quad \text{for} \quad j = l - k, \dots, l \quad (9)$$

$$d_j^{[m]} = (1 - \alpha_{m,j}) d_{j-1}^{[m-1]} + \alpha_{m,j} d_j^{[m-1]} \quad (10)$$

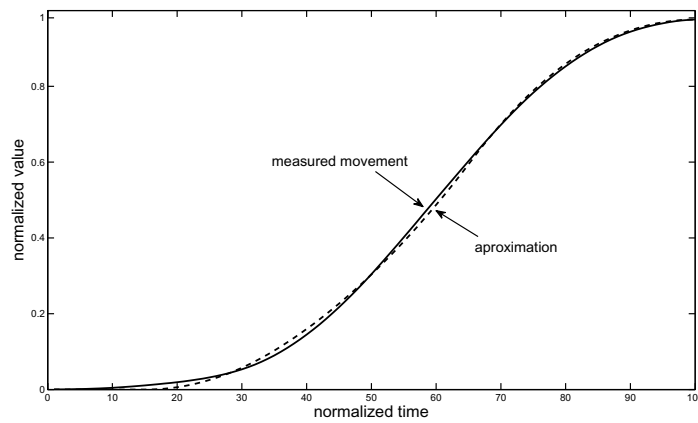
$$m = 1, \dots, k; \quad j = l - k + m, \dots, l \quad (11)$$

$$\alpha_{m,j} = \frac{x - x_j}{x_{j+k+1-m} - x_j} \quad (12)$$

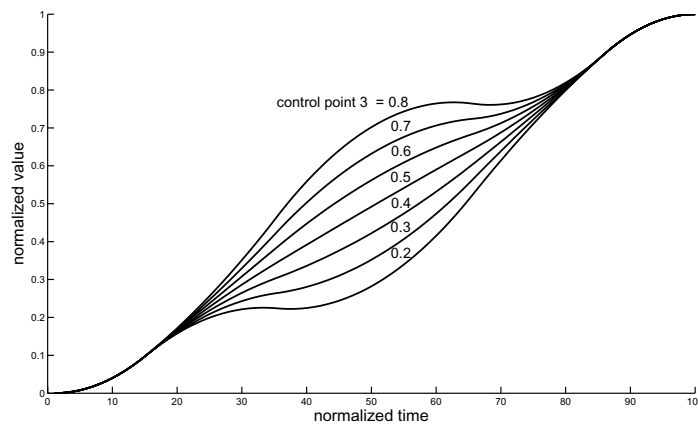
$$s(x) = d_1^{[k]}. \quad (13)$$



(a)



(b)



(c)

Fig. 3. (a) Five basic functions generated with B-splines. These functions are used in a simple approximation of movement from pick point to place point. (b) Measured movement and an approximation of arm movement. B-splines are used for approximation. (c) The influence of middle control point parametrization value  $d_3$  on the path of the arm trajectory. Five control points are used.

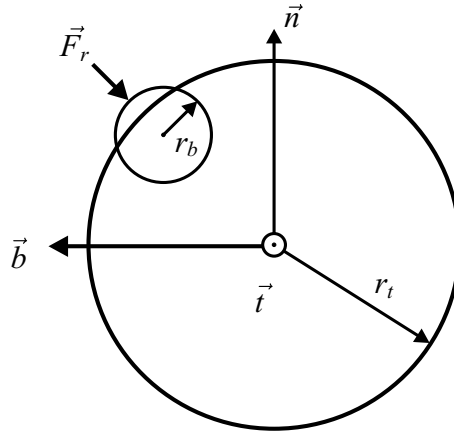


Fig. 4. Cross-section of the tunnel when the ball penetrates the wall of the tunnel. The reaction force  $\vec{F}_r$  is generated in the direction toward the central curve line.

Different number of control points can be used to describe the path of the arm from pick point to place point, depending on the complexity of the trajectory. Figure 3(a) shows five basic functions ( $j = 5$ ) when the trajectory is defined by five control points. An example of a healthy person measured movement and its corresponding approximation interpolated with B-splines are shown on Fig. 3(b). Figure 3(c) shows the influence of the middle control point (third control point  $d_3$  in case of five control points) on the trajectory path.

#### 2.4. The haptic trajectory tunnel

The approximated path using B-splines defines central curve line of the trajectory tunnel, linking the pick point and place point. This haptic trajectory tunnel also has the radius along the central curve line. The end point of the robot is haptically presented as a ball. The position of the ball is defined with the position of the robot end point while the size of the ball is minimal. The user can move the ball along the tunnel, as well as in radial direction when the ball diameter is smaller than the diameter of the tunnel. If the ball touches and penetrates the wall, the reaction force, which forces the ball out of the wall, is computed. Figure 4 shows a cross-section of the tunnel when the ball penetrates into the wall. Scalar  $r_t$  marks the radius of the tunnel and scalar  $r_b$  marks the radius of the ball.

The collision between the object and the tunnel wall is modeled as a spring-damper system with a stiffness  $k_r$  and viscous friction  $B_r$ . All forces are computed in the coordinate system of the tunnel, which is defined by a direction vector of the tangent on the central curve line  $\vec{t}$ , a direction vector of normal  $\vec{n}$  and a direction vector of binormal  $\vec{b}$ . Vector  $\vec{F}_r$  is the force of the tunnel wall while vector  $\vec{x}_{nb}$  is the penetration depth of the ball into the haptic wall. Vector  $\vec{v}_{nb}$  marks the velocity of the robot end point in  $\vec{n}\vec{b}$  plane.

$$\vec{F}_r = k_r \vec{x}_{nb} - B_r \vec{v}_{nb} \tag{14}$$

In addition to radial force  $\vec{F}_r$  an optional trajectory guidance force can be provided in the haptic trajectory tunnel. A reference time value defines the movement duration. The guidance force  $\vec{F}_g$  along tunnel central line is a spring-damper model with stiffness  $k_g$  and viscous friction  $B_g$ . Vector  $\vec{x}_t$  is the difference

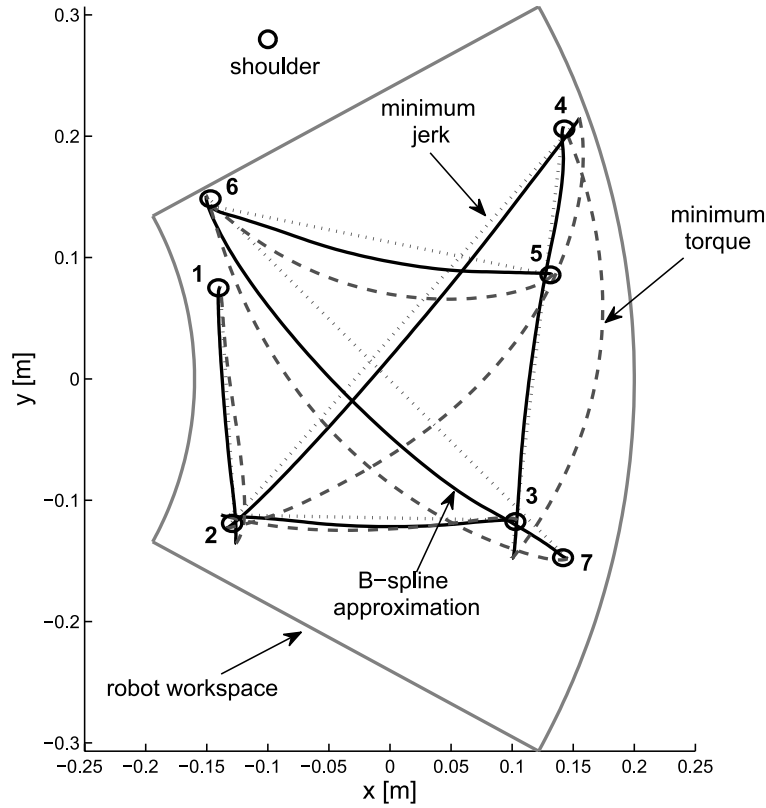


Fig. 5. Trajectory planning in  $\vec{x}\vec{y}$  plane with minimum jerk model, minimum torque model and approximation model using B-splines. Paths are shown for six different movements from start to end point (1→2, 2→3, 3→4, 5→6, 6→7, 4→2).

between a reference time position and the current end-effector position on the trajectory.  $\vec{v}_t$  represents the end-effector velocity in the direction of the tangent vector  $\vec{t}$ .

$$\vec{F}_g = k_g \vec{x}_t - B_g \vec{v}_t \quad (15)$$

The total force  $\vec{F}$  is the sum of two forces, the tunnel wall force and the guidance force.

$$\vec{F} = \vec{F}_r + \vec{F}_g \quad (16)$$

Described model of the haptic trajectory tunnel is designed as an object in the haptic Matlab/Simulink environment. Haptic tunnel is designed to be used as an independent haptic primitive. The path of the trajectory tunnel curve is defined by five control points for each dimension  $x$ ,  $y$  and  $z$ . The first and the fifth control point are the starting and final point of the tunnel. The normalized values of the other three control points are set in the mask of the model depending on the purpose of the task. The tunnel can be reset through an external parameter. After reset, the new start and end point of the trajectory tunnel are set. The subject can move from the current position to a new end placement point. The starting point is always the current position of the robot while an external parameter of the model sets the final point.

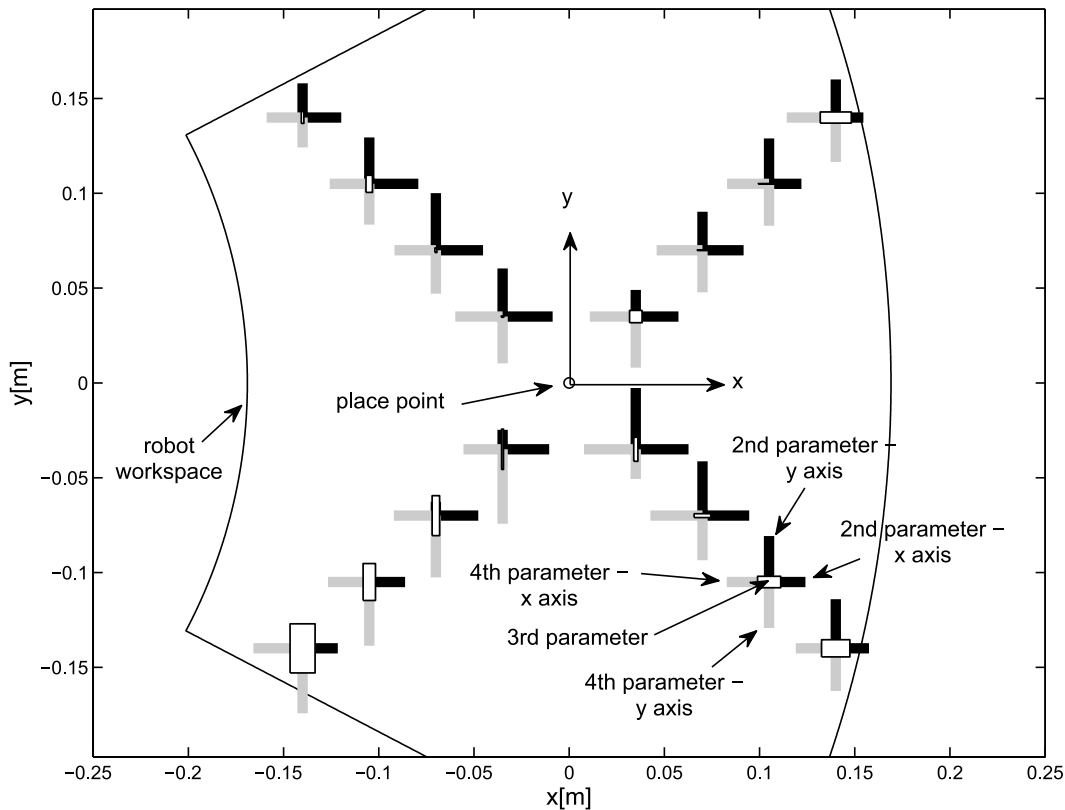


Fig. 6. Values of control points  $d_2$ ,  $d_3$  and  $d_4$  for movements in the  $\bar{x}\bar{y}$  plane for different movements in man arm workspace. The control point values are shown for each axis separately. The placing points of the healthy person movements were at the center of the coordinate system while the pick points were at marked places. The shoulder of the healthy subject is at the same position as in Fig. 6.

### 3. Results

In this section are shown results of the B-spline approximation based on measurements of movements in comparison to other two, minimum jerk and minimum torque approaches. Further, the trajectories with enabled haptic trajectory tunnel will be shown.

While Fig. 2 in methods section shows measured movements of healthy person in vertical plane with HapticMaster having zero impedance, Fig. 5 concentrates on the movements in a horizontal plane using three different path approaches. The healthy subject performed six point to point movements (1→2, 2→3, 3→4, 5→6, 6→7, 4→2) in the horizontal plane. The minimum jerk paths and the minimum torque paths are calculated analytically for the same six point to point movements. The dotted lines show minimum jerk paths while the hatched curves show minimum torque paths. The bold black curves show approximation paths generated with B-splines as described in the methods section.

To show that the human movements are repeatable and that the curvature of the movement depends on the direction and length of the pick to place point movement, we observed differences between the measured points and the linear path between pick and place points. From there were calculated average values of control points and then taken their absolute value for movement in a horizontal plane. These absolute values are differences of the measured control points values and the straight line control points

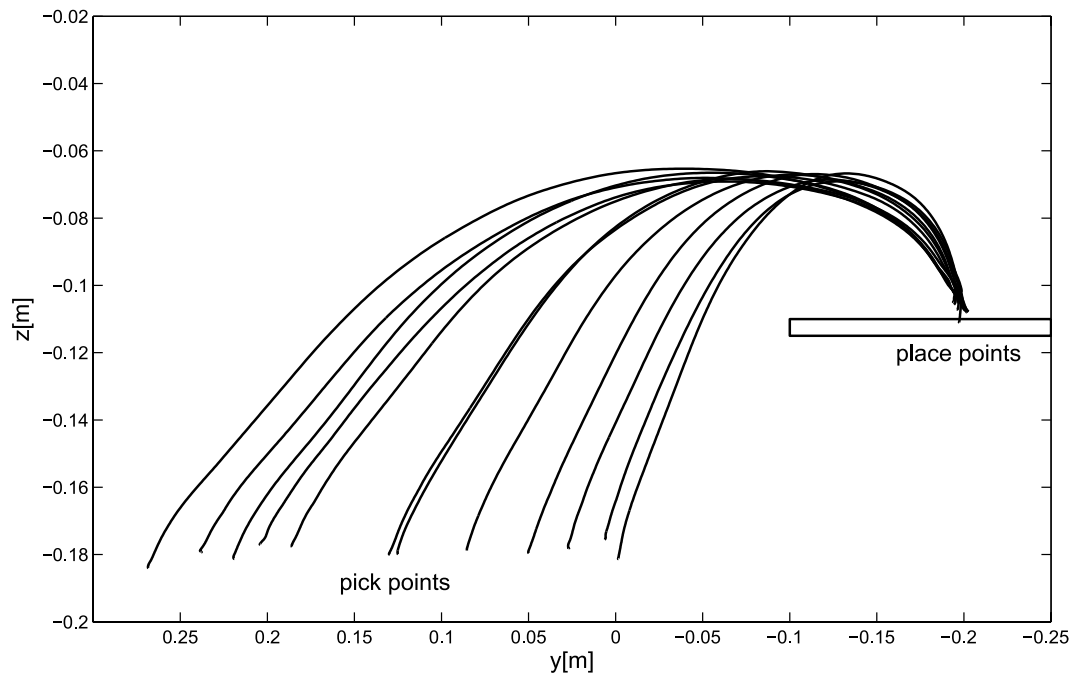


Fig. 7. Pick to place movements in the pick and place task with the haptic trajectory tunnel present. The experimenter was a healthy person and has to perform twelve movements.

values. The movements were performed by healthy subject in different directions. Figure 6 shows the absolute values of the middle three control points  $d_2$ ,  $d_3$  and  $d_4$  for different pick points in the  $xy$  plane. The solid black color marks value of the second control point  $d_2$ , the grey dotted color marks value of the fourth control point  $d_4$  while the white block marks the value of the third control point  $d_3$ . The place point of the trajectory was always in the center of the coordinate system. The absolute values of the control points  $d_2$ ,  $d_3$  and  $d_4$  are depicted at pick points in four directions. The second and fourth control point are divided into two parts, showing values in  $x$  and  $y$  direction respectively. The width of the white block represents the value of the third control point in  $x$  direction while the block height represents the value in  $y$  direction.

Figure 7 shows trajectories of movement from pick to place point using B-spline haptic tunnel. The trajectories were measured in healthy subject performing twelve pick to place movements. This task was performed under the same conditions as the task described in previous section (Fig. 2), only that the haptic trajectory tunnel was now present. Hemiparetic subject performed the same task in zero impedance space (Fig. 8) and with the haptic trajectory tunnel present (Fig. 9). The table height was lower and the movements lengths were shorter while the rest of experimental conditions were the same.

#### 4. Discussion

The new solutions in robot control enable use of haptic robots in rehabilitation environment. Trajectory planning is one of the crucial topics in rehabilitation robotics. How a human is planning the trajectory path of his arm? Most of the accessions explain that the human motor nerve system is subordinated by predefined rules [6,7,20,18]. Here is suggested the method, where movements measured in healthy people are used as a base for further trajectory planning.

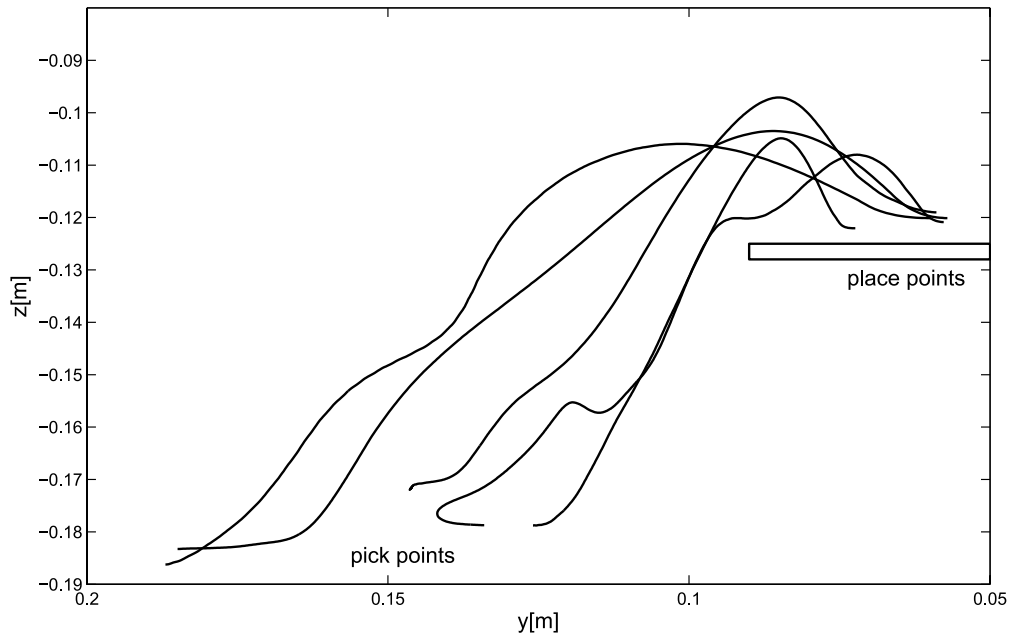


Fig. 8. Pick to place movements of the hemiparetic subject in the pick and place task in zero impedance space.

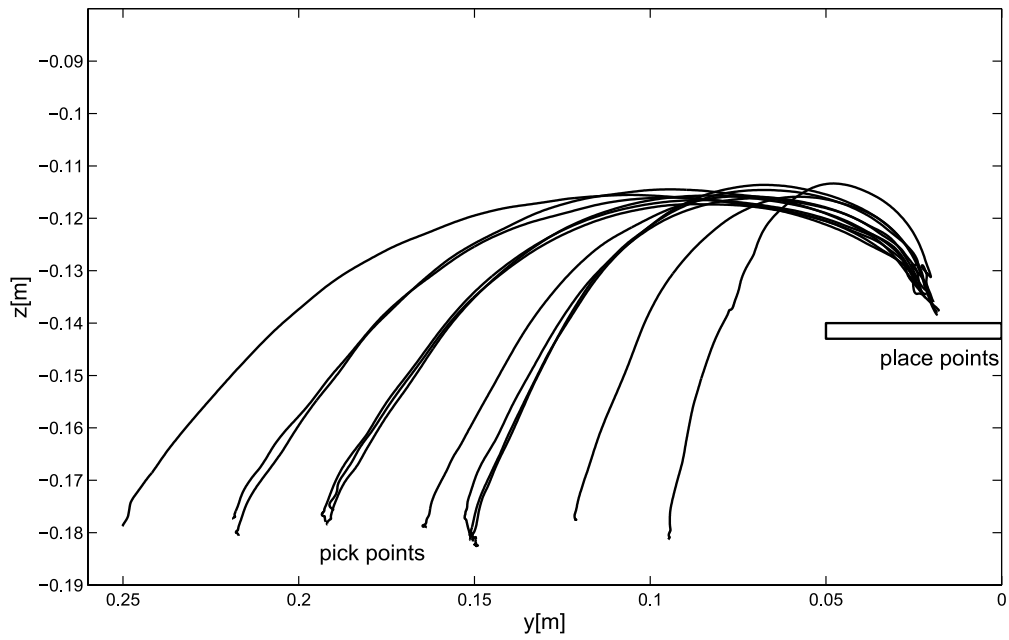


Fig. 9. Pick to place movements in the pick and place task with the haptic trajectory tunnel present. The user was a hemiparetic subject.

Different models of trajectory planning lead to different trajectories (Fig. 5) in a horizontal plane. The minimum jerk model generated straight lines between the points while the minimum torque model generated slightly curved lines. In cases where the direction of measured movement is forward or

backward (1→2, 3→4), the B-spline approximated trajectory is similar to the straight line while in other cases (2→3, 5→6, 6→7, 4→2), where the left and right movements are present, measured trajectory is similar to the minimum torque trajectory. Therefore, the B-spline approximated trajectory lies in most cases between paths of the comparable models. All the velocity profiles are bell-shaped, except in the minimum variance model, where the velocity curve slightly differs at the beginning and at the end of the movement.

To confirm that the human movements are repeatable, were initially examined the average absolute values of the middle three control points only by taking a number of measurements. Figure 6 shows that in the same directions values of the control points stay in the same proportion while the values decrease proportional with the length of the movements in all directions. These measurement findings confirmed that for similar pick and place points human movements are repeatable. It can be recognized from Figs 2 and 7 that the haptic trajectory tunnel determines the trajectory of the movement from the pick to the place point for a healthy subject. Our results showed that the pick to place trajectories of the patient under the same conditions with B-splines only slightly differ from the pick to place trajectories of the healthy person (Figs 7 and 9), while between healthy person and the patient the pick to place trajectories in zero impedance space evidently differ (Figs 2 and 8). Therefore, with the haptic trajectory tunnel, the patient is guided in cooperative manner to make same pick to place movements as healthy person with only minimal intervention from haptic system.

The big advantage of the presented trajectory planning method is primarily in the fact that the complexity of the movement being approximated does not play an important role. By using more control points, the method could be implemented also for other, much more complex trajectory planning problems, not only the point to point and pick to place movement. In the case of the pick to place movement, a typical curved trajectory in healthy person is present in  $z$  axis (Fig. 7). The point to point movements of different models on Figs 5 and 6 were focused in the  $\vec{x}\vec{y}$  plane. However, the findings in the  $\vec{x}\vec{y}$  plane can be further extended to  $z$  axis for movement from point to point. Similar observations are valid for path trajectories in hemiplegic person, while using B-splines paths and haptic tunnel.

## 5. Conclusion

Goal of this study was to create a trajectory planning algorithm and to develop adequate haptic object. The algorithm exploits use of the movements measured in healthy people as a base for further trajectory planning in patients. The results showed that approximated movements represent the paths that lie between minimum jerk paths and minimum torque paths depending on movement direction. In the same directions, the values of the control points stay in the same proportion while the values decrease proportional with the length of the movements in all directions. The measurement findings confirmed that for similar pick and place points human movements are repeatable. Further, a haptic object, which helps the patient to move along the minimum intervention trajectory was designed. The results of our simple task confirmed that the patient can make same pick to place movements as healthy person when using the trajectory tunnel. These findings show that our model, which uses B-splines and haptic tunnel together with other movement primitives, can be easily implemented in rehabilitation robotics. Our next step is inclusion of the tunnel in an upper extremity robotic therapy system.

## References

- [1] J.M. Alho, Scenarios, uncertainty and conditional forecast of the world population, *Journal of the Royal Statistical Society: Series A (Statistics in Society)* **160** (1997), 71–85.

- [2] Amer. Heart Assoc., Heart and stroke statistical update, *Circulation* **117** (2008), 25–146.
- [3] A. Deneve, S. Moughamir, L. Afilal and J. Zaytoon, Control system design of a 3-DOF upper limbs rehabilitation robot, *Computer Methods and Programs in Biomedicine* **89** (2008), 202–214.
- [4] D. Erol and N. Sarkar, Coordinated control of assistive robotic devices for activities of daily living tasks, *IEEE Transactions on Neural Systems and Rehabilitation Engineering* **16** (2008), 278–285.
- [5] G. Farin, *Curves and Surfaces for CAGD*, Morgan Kaufmann, 2001.
- [6] P.M. Fitts, The information capacity of the human motor system in controlling the amplitude of movement, *Journal of Experimental Psychology* **121** (1992), 262–269.
- [7] T. Flash and N. Hogan, The coordination of arm movements: an experimentally confirmed mathematical model, *The Journal of Neuroscience* **5** (1985), 1688–1703.
- [8] A. Frisoli, F. Rocchi, S. Marcheschi, A. Dettori, F. Salsedo and M. Bergamasco, A new force-feedback arm exoskeleton for haptic interaction in virtual environments, in: *Eurohaptics Conf. and Symp. on Haptic Interfaces for Virtual Environment and Teleoperator Systems*, Pisa, 2005, 195–201.
- [9] J. He, E.J. Koeneman, R.S. Schultz, D.E. Herring, J. Wanberg, H. Huang, T. Sugar, R. Herman and J.B. Koeneman, RUPERT: a Device for Robotic Upper Extremity Repetitive Therapy, in: *27th Annu. Int. Conf. of the Engineering in Medicine and Biology Society*, Shanghai, 2005, 6844–6847.
- [10] N. Hogan, H.I. Kerbs, J. Charannarong, P. Srikrishna and A. Sharon, MIT – MANUS: A workstation for manual therapy and training I, in: *IEEE Int. Workshop on Robot and Human Communication*, Tokyo, 2005, 161–165.
- [11] P.S. Lum, C.G. Burgar and P.C. Shor, Evidence for improved muscle activation patterns after retraining of reaching movements with the MIME robotic system in subjects with post-stroke hemiparesis, *IEEE Transactions on Neural Systems and Rehabilitation Engineering* **12** (2004), 184–194.
- [12] R.C.V. Loureiro and W.S. Harwin, Reach & Grasp Therapy: Design and Control of a 9-DOF Robotic Neuro-rehabilitation System, in: *IEEE 10th Int. Conf. on Rehabilitation Robotics*, Kyoto, 2007, 757–763.
- [13] M. Mihelj, T. Nef and R. Reiner, A novel paradigm for patient-cooperative control of upper-limb rehabilitation robots, *Advanced Robotics* **21** (2007), 843–867.
- [14] T. Nef, M. Mihelj, G. Kiefer, C. Perndl, R. Müller and R. Reiner, ARMin – Exoskeleton for arm therapy in stroke patients, in: *IEEE 10th Int. Conf. on Rehabilitation Robotics*, Noordwijk, 2007, 68–74.
- [15] J.C. Perry, J. Rosen and S. Burns, Upper-Limb Powered Exoskeleton Design, *IEEE Transactions on Mechatronics* **12** (2007), 408–417.
- [16] J. Podobnik, M. Munih and J. Cinkelj, Hand and arm rehabilitation system, in: *Int. Conf. on Disability, Virtual Reality and Associated Technologies*, Maia, 2008, 237–244.
- [17] B. Siciliano and O. Khatib, *Springer Handbook of Robotics*, Springer, 2008.
- [18] G. Simmons and Y. Demiris, Optimal robot arm control using the minimum variance model, *Journal of Robotic Systems* **22** (2005), 677–690.
- [19] A. Sunderland, D.J. Tinson, E.L. Bradley, D. Fletcher, R. Langton Hewer and D.T. Wade, Enhanced physical therapy improves recovery of arm function after stroke. A randomised controlled trial, *Journal of Neurology, Neurosurgery, and Psychiatry* **55** (1992), 530–535.
- [20] Y. Wada, Y. Kaneko, E. Nakano, R. Osu and M. Kawato, Quantitative examinations for multi joint arm trajectory planning – using a robust calculation algorithm of the minimum commanded torque change trajectory, *Neural Networks* **14** (2001), 381–393.
- [21] E.T. Wolbrecht, J. Leavitt, D.J. Reinkensmeyer and J.E. Bobrow, Control of a pneumatic orthosis for upper extremity stroke rehabilitation, in: *IEEE Engineering in Medicine and Biology Conf.*, New York, 2006, 2687–2693.
- [22] L.Q. Zhang, H.S. Park and Y. Ren, Developing An Intelligent Robotic Arm for Stroke Rehabilitation, in: *Proc. of the IEEE 10th Int. Conf. on Rehabilitation Robotics*, Noordwijk, 2007, 984–994.